PAPER

Unexpected bond activations promoted by palladium nanoparticles†

A. M. López-Vinasco,[a] I. Favier,[b,c] C. Pradel,[b,c] L. Huerta,[d] I. Guerrero-Ríos,[a] E. Teuma,[b,c] M. Gómez*[b,c] and E. Martin*[a]

Thioether-phosphines, **1** and **2**, were applied for the stabilisation of palladium nanoparticles (PdNPs) synthesised by a bottom-up methodology, using [Pd$_2$(dba)$_3$] as an organometallic precursor. For the phenyl containing ligand **1**, small (d_{mean} = 1.6 nm), well-defined and dispersed nanoparticles were obtained; however, ligand **2** involving a long alkyl chain led to agglomerates. NMR and GC-MS analyses throughout the synthesis of the nanomaterials revealed partial cleavage of ligands by C–S and C–P bond activations, and XPS spectra of the isolated nanoparticles indicated the presence of both thioether-phosphines and their fragments on the metallic surface. Reactivity studies of molecular palladium systems as well as on extended palladium surfaces pointed out that cluster entities are responsible for C-heteroatom activations, triggering structure modifications of stabilisers during the synthesis of PdNPs.

Introduction

The decomposition of organometallic precursors under appropriate conditions represents an elegant synthetic method to form metallic nanoparticles with a well-defined composition and controlled morphology.[1] This bottom-up methodology frequently uses macromolecules as stabilisers, for instance polymers, dendrimers or surfactants.[2] Molecular ligands are also suitable due to their coordinative abilities as well as for the possible tuning of electronic and steric properties of the metallic surface,[3] especially relevant for catalytic purposes.[4] However, the interaction of heteroatoms, such as nitrogen, oxygen, phosphorus or sulphur, with the metallic surface can trigger ligand modification by bond activation processes.

In relation to C–S bond cleavages, most reported studies concern activations promoted by molecular transition metal complexes.[5] Thiophenes and related derivatives have been extensively studied as model substrates for hydrodesulfurization processes.[6] Recently, this type of bond ruptures involving thioethers have attracted attention,[7] in particular for their potential applications in synthetic chemistry.[8] Additionally, metallic clusters, such as those of Pt[9] and MoS$_2$,[10] as well as Ni[11] and Au[12] surfaces, have proven capable of splitting C–S bonds when thiophenes and thiols are involved. Moreover, copper nanoclusters containing thiolates, [Cu$_n$(SR)$_m$], generated Cu$_2$S nanodiscs by thermal treatment.[13]

Although C–P bond activations mediated by transition metals are less favoured than those corresponding to C–S cleavages, metal–phosphide nanoparticles were prepared by direct reaction of the corresponding metal with alkyl-phosphanes at high temperatures, by means of activation of C–P bonds, such as for InP and FeP nanoparticles.[14] C–P cleavages could be also promoted by molecular clusters under thermal or photochemical conditions, for instance those based on Mo,[15] Ru,[16] Os,[17] Mn and Re.[18] Interestingly, both C–S and C–P sequential bond activations of furyl- and thienyl-phosphines led to the formation of triruthenium clusters.[19]

Taking into account these precedents, we wondered whether coordinating ligands employed as stabilisers for metallic nanoparticles could be modified during their synthesis starting from molecular precursors. Therefore, we became interested in identifying the nature of ligands interacting with palladium nanoparticles (PdNP).

Herein, we describe the synthesis of new PdNP stabilised by thioether-phosphines. The observed reactivity of these ligands during the PdNP formation was compared to that using both molecular and heterogeneous palladium sources, with the aim of understanding the palladium mediated C–S and C–P bond activations.

[a]Depto. de Química Inorgánica, Facultad de Química, Universidad Nacional Autónoma de México, Av. Universidad 3000, 04510 D.F., México. E-mail: erikam@unam.mx; Fax: +52 55 5622 3720
[b]Université de Toulouse, UPS, LHFA, 118 route de Narbonne, 31062 Toulouse cedex 9, France
[c]CNRS, LHFA UMR 5069, 31062 Toulouse cedex 9, France. E-mail: gomez@chimie.ups-tlse.fr; Fax: +33 5 6155 8204; Tel: +33 5 6155 7738
[d]Instituto de Investigaciones en Materiales, Universidad Nacional Autónoma de México, Apartado Postal 70-360, México D.F. 04510, México. Fax: +52 55 5622 4715
†Electronic supplementary information (ESI) available: Syntheses of XPS reference materials and Fig. S1–S15 and Tables S1–S2. See DOI: 10.1039/c3dt53649a
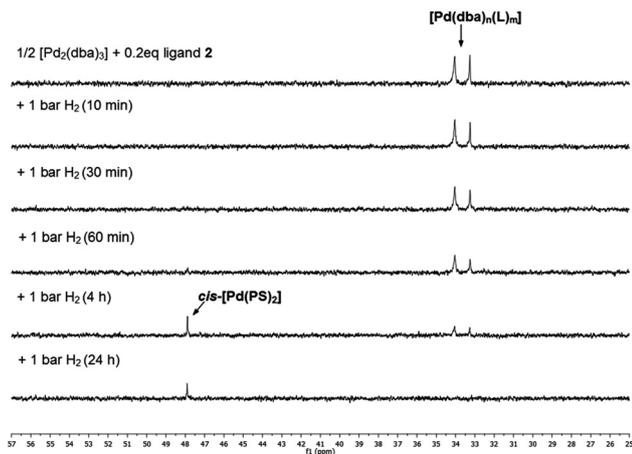
Results and discussion

Synthesis and characterization of PdNP

PdNP containing thioether-phosphines were synthesised from $[Pd_2(dba)_3]$ in the presence of the corresponding ligand (**1** or **2**) under H_2 pressure (Scheme 1) following the methodology previously described.[1a] TEM analyses proved the significant effect of the nature of the ligand on the material. While ligand **1** led to small (1.6 ± 0.5 nm), well-defined and dispersed nanoparticles (Fig. 1a), ligand **2** merely gave agglomerates (Fig. 1b). The satisfactory stabilisation of **PdNP1** may be related to the π-aromatic interaction with the metallic surface besides the donor ability of the heteroatoms.[3a] Intriguingly, the behaviour displayed by **PdNP2** is different from what could be expected, given that stabilisers containing long alkyl chains frequently act as surfactants favouring dispersion between nanoparticles.[20]

IR spectra of both **PdNP1** and **PdNP2** materials evidenced the presence of aromatic ligands, THF and dibenzylidenacetone and/or its C=C bond hydrogenated product (Fig. S1 and S2†). In particular, two strong bands, present in both ligand spectra, at 746 and 698 cm^{-1}, were also observed for the corresponding palladium nanoparticles; these bands are attributed to the out-of-plane deformation for mono- and di(*ortho*)-substituted phenyl compounds. THF at the metallic surface could be evidenced by strong absorptions in the range 1300–1000 cm^{-1}. Weaker absorptions at *ca.* 1630 cm^{-1} could be assigned to dibenzylidenacetone and its partially reduced compound.

Surprisingly, GC-MS analyses of the organic phases coming from the reaction mixtures revealed the presence of benzene in the case of **PdNP1** (Fig. S3†) and decane and decylphenyl-thioether for **PdNP2** (Fig. S4†). It is important to note that not

more than 30% of ligand degradation was observed under the conditions employed for the synthesis of both nanoparticles, **PdNP1** and **PdNP2**.

With the aim of verifying the nature of the stabilisers present on the metallic surface after the isolation of the materials, ligand exchange reactions of the as-prepared PdNP were tested using both carbon monoxide and dodecanethiol (Scheme 2). None permitted to replace the stabilisers on the metallic surface even after one week of reaction. In addition, when palladium nanoparticles were treated under aerobic reflux of toluene, triphenylphosphine oxide (O=PPh$_3$) was recovered as the only product, pointing to C$_{aryl}$–S bond activation for both **PdNP1** and **PdNP2**. It is important to note that free ligands **1** and **2** under the same aerobic conditions exclusively gave the corresponding thioether-phosphine oxides, without any sign of cleavage bonds.

When **PdNP2** was reacted with concentrated nitric acid at room temperature, O=PPh$_3$ and **2** were mainly obtained, together with a small amount of thioether-phosphine oxide. Free ligand **2** treated with nitric acid showed low reactivity, partially giving the thioether-phosphine oxide without the formation of O=PPh$_3$. These indirect analyses proved that ligand **2** was present at the metallic surface. An analogous study carried out with **PdNP1** only indicated the presence of O=PPh$_3$ even for the reaction of free ligand **1** with nitric acid,

Scheme 1 Synthesis of palladium nanoparticles **PdNP1** and **PdNP2**, stabilised by thioether-phosphines **1** and **2** respectively.

Scheme 2 Surface reactivity for **PdNP1** and **PdNP2** (L$_{frag}$ means fragments of thioether-phosphines coming from C−P and/or C−S bond activation).

Fig. 1 TEM images of **PdNPL** corresponding to: **PdNP1** with their size distribution histogram (a); **PdNP2** (b).

Fig. 2 ^{31}P NMR monitoring during the formation of **PdNP2**.

in the absence of palladium. The high reactivity of **1** under oxidative conditions makes it difficult to prove the presence of ligand **1** on the metallic surface.

As a result, a plausible PdNP degradation during the tests to release the thioether-phosphine ligand from the metallic surface could be presumed, but ligand degradation during the synthesis of PdNP cannot be ruled out.

In order to identify the organic and organometallic species involved in the formation of **PdNP1** and **PdNP2**, the syntheses were carried out in THF-d_8 at NMR Young tube scale, allowing ^{31}P and ^1H NMR monitoring; the corresponding organic phases were also analysed by GC-MS.

When [Pd$_2$(dba)$_3$] and L (**1** or **2**) were mixed in the absence of H$_2$ (Pd/L ratio = 1/0.2), two signals appeared in ^{31}P NMR spectra at *ca.* 31–34 ppm for both systems (Fig. 2 for the Pd/**2** system and Fig. S5† for the Pd/**1** system), which could be attributed to thioether-phosphine containing Pd(0) species [Pd(dba)$_n$(L)$_m$] according to reported data for related compounds.[21] Under dihydrogen pressure, the intensity of signals decreased and a new signal of low intensity appeared at

48 ppm after 1 h, assigned to the palladium(II) complex *cis*-[Pd-(PS)$_2$] (PS represents the anionic ligand Ph$_2$P–(2-S–C$_6$H$_4$)).[22] This compound was formed by C$_{aryl}$–S (ligand **1**) and C$_{alkyl}$–S (ligand **2**) bond activations, *via* oxidative addition of the SR moiety to Pd(0) followed by R–H reductive elimination (R = C$_6$H$_5$, C$_{10}$H$_{21}$), giving benzene and decane for **1** and **2**, respectively. After 1 h for **PdNP1** and after 4 h for **PdNP2**, under H$_2$ pressure, signals corresponding to Pd(0) molecular species practically disappeared, in agreement with the formation of nanoparticles.

GC-MS analysis of the organic phase evidenced the presence of benzene for **PdNP1** and both decane and decylphenylthioether for **PdNP2** as observed in the synthesis of PdNP (see above). These facts indicate that not only C–S bond activations (C$_{aryl}$–S and C$_{alkyl}$–S) but also C–P bond cleavages take place. In contrast, for **PdNP1**, no diphenylthioether was observed. The formation of secondary phosphines, such as HPPh$_2$ and HPPh(2-SR–C$_6$H$_4$) (where R = Ph, decyl), or the corresponding phosphides species could not be excluded. Neither these phosphorus species nor their corresponding molecular metal complexes were observed; therefore, it is reasonable to assume their presence on the metallic surface.

XPS survey spectra for both materials **PdNP1** and **PdNP2** showed the presence of palladium, sulphur, carbon and oxygen, but unfortunately phosphorus could not be detected (Fig. S6†); the presence of phosphorus was evidenced by EDX analyses for both nanomaterials (Fig. S7 and S8† for **PdNP1** and **PdNP2**, respectively). Analyses of high-resolution spectra in the binding region corresponding to Pd 3d$_{5/2}$ and Pd 3d$_{3/2}$ (Fig. 3, Table S1†) permitted us to propose the presence of Pd(II) species coordinated to sulphide and thiolate species (SPh and PS, respectively) for **PdNP1** and both SC$_{10}$H$_{21}$ and PS anions for **PdNP2**, in addition to the main Pd(0) species. This behaviour is in agreement with that observed for PdNPs just stabilised by [BMI][PF$_6$] (BMI = *n*butyl-methyl-imidazolium) where Pd(0) and Pd(II) chemical states were observed on the metallic surface by XPS studies; the major contribution corresponds to Pd(0) as deduced from the binding energy region of
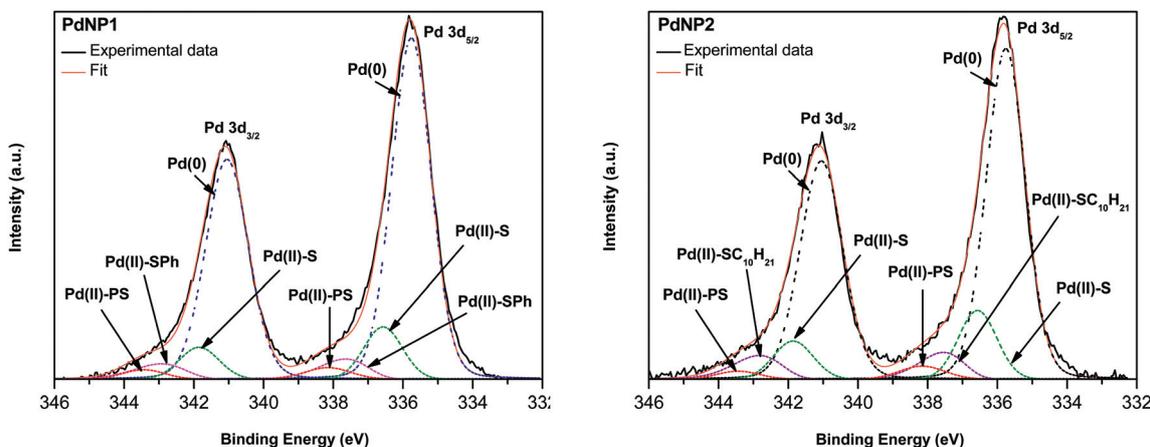

Fig. 3 High-resolution XPS spectra of the Pd 3d binding region for **PdNP1** (left) and **PdNP2** (right).

Pd 3d.[23] Deconvolutions of the experimental signals were based on PdS, $[Pd(SPh)_2]_n$, $[Pd(SC_{10}H_{21})_2]_n$ and cis-$[Pd(PS)_2]$ as Pd(II) references, and bulk palladium as the Pd(0) pattern (Fig. S9 and S10†). Pd(0) species containing phosphines, such as $[Pd(PPh_3)_4]$, also exhibit binding energies in the regions corresponding to the bulk metal.[24]

Analyses of high-resolution spectra in the binding region corresponding to S $2p_{3/2}$ proved the presence of the thioether-phosphine ligands **1** and **2**, corroborating also the contributions of sulphide and thiolate species, according to the previously reported data.[25] For a full analysis, deconvolutions of the experimental signals were also based on $[PdCl_2(L)]$ (where L = **1**, **2**), PdS, $[Pd(SPh)_2]_n$, $[Pd(SC_{10}H_{21})_2]_n$ and cis-$[Pd-(PS)_2]$ (Fig. S11 and S12, Table S2†).

To more fully understand the nature of the palladium species responsible of the observed carbon–heteroatom bond activations, the reactivity of molecular and extended surface palladium systems was envisaged.

Molecular and extended surface reactivity

Concerning the molecular reactivity, ^{31}P NMR monitoring of THF mixtures of $[Pd_2(dba)_3]$ and L (Pd/L ratio = 1/0.2) in the absence of dihydrogen displayed the formation of molecular Pd(0) species coordinated to the thioether-phosphine ligands (Fig. S13 and S14† for **1** and **2**, respectively).

Complexes containing **1** evolved from purple to dark solutions with the disappearance of initial NMR signals. After 4 h, a low intensity signal at 52 ppm emerged, indicating the formation of Pd(II) thiolate species trans-$[Pd(PS)_2]$, the kinetically-controlled isomer;[22] accordingly, benzene was detected in the organic phase (Fig. S15†). In contrast, ^{31}P NMR spectra for the mixture $[Pd_2(dba)_3]$ with **2** did not show any signal changes after 24 h. These results, obtained in the absence of dihydrogen, indicate that only the Pd/**1** system led to the formation of heterogeneous entities. Its behaviour suggests that the C–S bond activation is induced by metallic heterogeneous species and, consequently, palladium leaching promoted by phosphine-thiolates takes place (trans-$[Pd(PS)_2]$).

In relation to surface reactivity, Pd/C was chosen as the model material. Thioether-phosphines in the presence of Pd/C in THF under H_2 (3 bar) at room temperature led to ca. 7% degradation of ligands. GC-MS analyses of the organic phases evidenced the formation of diphenylthioether and decylphenyl-thioether for **1** and **2** respectively, resulting from C–P bond activation (ca. 2%). The corresponding products originating from C_{aryl}–S and C_{alkyl}–S bond activations (ca. 5%), benzene (for ligand **1**) and decane (for ligand **2**), were also detected.

Conclusions

In summary, we could prove that the thioether-phosphine **1** containing a phenyl moiety on the sulphur atom is able to give small and well-dispersed nanoparticles. In contrast, ligand **2** leads to the formation of agglomerates.
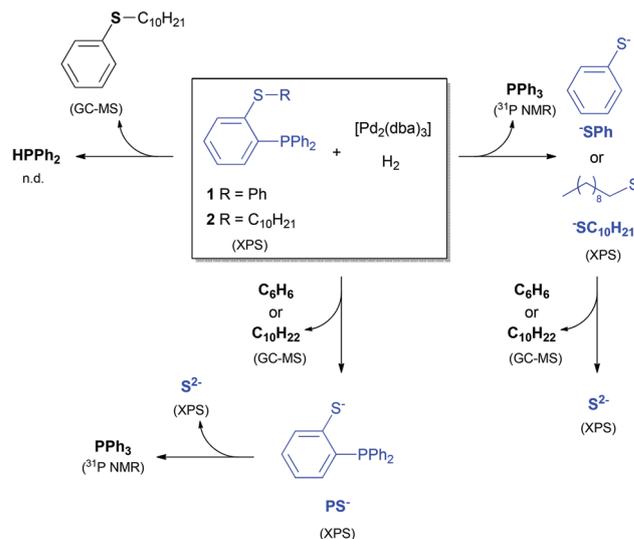
Scheme 3 Partial cleavage of thioether-phosphine ligands promoted by Pd(0). In blue, species present on the metallic surface. Detection techniques are shown in brackets (n.d = not detected).

XPS analyses of the as-prepared materials evidenced the presence of thioether-phosphines and the corresponding thiolate and sulphide fragments at the metallic surface. Additionally, GC-MS analyses from the organic phases corresponding to the synthesis of PdNP displayed the formation of the organic compounds coming from C–S and C–P bond activation processes, under dihydrogen pressure at room temperature. In Scheme 3, the different C-heteroatom bond cleavages produced during the synthesis of PdNP are summarised.

A thorough analysis during the synthesis of palladium nanoparticles by means of ^{31}P NMR and GC-MS techniques suggested that metallic surfaces trigger the cleavage of C-heteroatom bonds, in agreement with the reactivity observed using Pd/C.

This work demonstrates the high reactivity of the metallic species generated from decomposition of molecular precursors during the synthesis of nanoparticles, modifying the stabiliser structure and able to induce significant consequences for the applications of the nanomaterials, in particular in catalysis.

Experimental

General

All manipulations of air- and moisture-sensitive compounds were performed under a dry nitrogen or argon atmosphere using standard Schlenk and vacuum-line techniques. Reagents were purchased from commercial providers and used without further purification. The organic solvents were purified by standard procedures and distilled under nitrogen. Thioether-phosphine ligands **1** and **2** were prepared following literature methods.[26,27] NMR spectra were recorded on a Varian (Unity Inova) 300 and on a Bruker Avance 300 (300 MHz for ^{1}H NMR and 121 MHz for ^{31}P NMR). TEM images were obtained using

a transmission electron microscope JEOL JEM 1400 running at 120 kV. EDX spectra were recorded on a JEOL JEM-2010 running at 120 kV coupled to an Oxford ISIS or a Thermoscientific detector. FT-IR spectra were recorded on a Perkin Elmer FT-IR 1605 spectrophotometer. GC-MS analyses were performed on: (a) a Perkin-Elmer Clarus 500 chromatograph equipped with an FID, an MS-detector and an SGE BPX5 capillary column; and (b) a Thermo-Electron Trace GC Ultra fitted with an FID, an MS-detector, and a DB-5MS capillary column. XPS measurements were performed using a VG Microtech ESCA2000 Multilab UHV system with an Al K_α X-ray source ($h\nu$ = 1486.6 eV) and a CLAM4 MCD analyser. XPS spectra were obtained at 55° from the normal surface in the constant pass energy mode (CAE), E_0 = 50 and 20 eV for survey and high resolution narrow scan. Peak positions were referenced to the Shirley background Ag $3d_{5/2}$ core level at 368.20 eV, Au $4f_{7/2}$ at 84.00 eV and C 1s hydrocarbon groups at 285.00 eV central peaks. XPS spectra were fitted with the program SDP v 4.1.[28] The atomic relative sensitivity factor (RSF) reported by Scofield was corrected by a transmission function of the analyser.[29] XPS spectra of Pd 3d and S 2p core levels showed spin–orbit coupling, and the doublet separation was set to 1.21 eV and 5.29 eV. XPS error is based on considering a detection limit estimated to be 0.1% in mass and uncertain propagation. For the deconvolution analysis the uncertainty was estimated at 5% of the binding energy. Deconvolution analyses were done using reference materials: synthesis and characterisation of [PdCl$_2$**2**] and [Pd(SC$_{10}$H$_{21}$)$_2$]$_n$ are described in ESI;† [PdCl$_2$**1**],[26] [Pd(SPh)$_2$]$_n$,[30] cis/trans-[Pd(PS)$_2$][22] and PdS were prepared as reported in the literature. The Pd(0) component was referenced using the values reported in the literature for [Pd(PPh$_3$)$_4$],[24a] elemental palladium[24b,c] and Pd(0)NPs.[31]

General procedure for the synthesis of palladium nanoparticles PdNPL (L = 1, 2). [Pd$_2$(dba)$_3$]·CHCl$_3$ (0.0870 mmol, 80 mg) and the appropriate ligand (0.0174 mmol, ratio Pd : L = 1 : 0.2) were placed in a Fisher-Porter bottle. THF (80 mL) dried and degassed was introduced under an argon atmosphere. The system was then pressurized with H$_2$ (3 bar) and stirred at room temperature overnight, leading to a black suspension. After replacing the residual H$_2$ pressure by argon, a sample was taken for TEM and GC-MS analyses. THF was removed under reduced pressure and the remaining solid was washed with pentane (3 × 10 mL) and dried under reduced pressure. The organic phase was concentrated and analysed by ^{1}H NMR proving the absence of free ligand.

General procedure for ^{31}P NMR monitoring of PdNPL formation (L = 1, 2). An NMR tube (Wilmad NMR tube w/J. Young valve, 5 mm) was charged with [Pd$_2$(dba)$_3$]·CHCl$_3$ (0.0132 mmol, 13.71 mg) and the appropriate ligand (0.0026 mmol, ratio Pd : L = 1 : 0.2) and connected to a vacuum line. THF (0.6 mL) dried and degassed was transferred under an argon atmosphere and stirred manually and the ^{31}P NMR spectrum was recorded. The system was then pressurized with H$_2$ (1 bar) and stirred manually at room temperature. ^{31}P NMR spectra were recorded every 10 minutes during the first hour and at 4, 6 and 24 h. Formation of PdNP was presumed after

1 h due to the intensity decrement of complex signals and the gradual change from a dark red solution to a black suspension. The complex cis-[Pd(PS)$_2$] was prepared in order to assign the signal in ^{31}P NMR at 48 ppm according to the literature method.[22]

General procedure for the identification of Pd molecular species at a Pd : L ratio of 1 : 0.2. An NMR tube (Wilmad NMR tube w/J. Young valve, 5 mm) was charged with [Pd$_2$(dba)$_3$]·CHCl$_3$ (0.0120 mmol, 12.42 mg) and the appropriate ligand (0.0024 mmol, ratio Pd : L = 1 : 0.2) and connected to a vacuum line. THF (0.6 mL) dried and degassed was transferred under an argon atmosphere and the system was manually stirred at room temperature. ^{31}P NMR spectra were recorded at different time intervals. The complex trans-[Pd(PS)$_2$] was prepared in order to assign the signal in ^{31}P NMR at 52 ppm according to the literature method.[22]

Procedure for ligand exchange reactions of PdNP1 with CO and dodecanethiol (DDT). An NMR tube (Wilmad NMR tube w/J. Young valve, 5 mm) was charged with **PdNP1** (ca. 10 mg) and the appropriate deuterated solvent (0.6 mL, THF-d_8 for CO and CD$_2$Cl$_2$ for DDT) and connected to a vacuum line. The corresponding ligand, CO (3 bar) and DDT (0.0786 mmol, 18.8 μL, **1** : DDT ratio = 1 : 3) were added under an argon atmosphere and stirred manually. ^{31}P NMR spectra in the case of CO presence were recorded at 1 h, 24 h, 3 and 7 days, whereas for the experiment in the presence of DDT, ^{1}H and ^{31}P NMR spectra were recorded at 2 h, 48 h, 5 days, 7 days and 3 weeks.

General procedure for the thermal treatment of PdNPL and ligands with Pd/C (L = 1, 2). PdNPL (ca. 10 mg) and toluene (10 mL) were placed in a flask. Similarly, the appropriate thioether-phosphine ligand **1** or **2** (0.0461 mmol, Pd : L ratio 0.2), Pd/C 10% (0.2349 mmol Pd, 0.25 g) and toluene (15 mL) were placed in a flask. The system was stirred at reflux temperature for 24 h. The solution was filtered over celite and the remaining solution was concentrated at reduced pressure. The residue was analysed by ^{31}P NMR and GC-MS.

Oxidative treatment of PdNPL and ligands using nitric acid. Distilled water (1 mL) was added to **PdNPL** (ca. 10 mg) or the appropriate ligand (for **1**: 10 mg, 0.027 mmol; for **2**: 6 mg, 0.014 mmol) was placed in a flask and cooled with an ice bath; nitric acid (conc. 68%) was slowly added (2 mL) and the solution was stirred for 20 h at room temperature. The aqueous solution (orange for PdNP and colourless for L) was then extracted with CH$_2$Cl$_2$ (1 mL). The organic phase was washed with water in order to eliminate the remaining acid and then analysed by GC headspace in the case of ligands, GC/MS and ^{31}P NMR for both PdNP and ligands.

General procedure for the hydrogenation treatment of ligands using Pd/C. The appropriate thioether-phosphine ligand **1** or **2** (0.094 mmol, Pd : L ratio = 1 : 0.2), Pd/C 10% catalyst (0.4698 mmol Pd, 0.5 g) and THF (20 mL) were placed in a 45 mL stainless steel autoclave equipped with a magnetic stirrer. The system was then pressurized with H$_2$ (3 bar) and stirred for 18 h at room temperature. Then, organic phases were separated and analysed by GC-MS.

Acknowledgements

Notes and references

1 For selected contributions, see: (a) K. Philippot and B. Chaudret, *C. R. Chim.*, 2003, **6**, 565; (b) I. Favier, E. Teuma and M. Gómez, *C. R. Chim.*, 2009, **12**, 533.

2 For selected contributions, see: (a) A. Roucoux, J. Schulz and H. Patin, *Chem. Rev.*, 2002, **102**, 3757; (b) *Metal Nanoparticles: Synthesis, Characterization and Applications*, ed. D. L. Feldheim and C. A. Foss, Jr., Marcel Deker, New York, 2002; (c) D. Astruc, F. Lu and J. Ruiz Aranzaes, *Angew. Chem., Int. Ed.*, 2005, **44**, 7852.

3 For selected coordination studies at the metallic surface, see: (a) I. Favier, S. Massou, E. Teuma, K. Philippot, B. Chaudret and M. Gómez, *Chem. Commun.*, 2008, 3296; (b) I. Favier, P. Lavedan, S. Massou, E. Teuma, K. Philippot, B. Chaudret and M. Gómez, *Top. Catal.*, 2013, **56**, 1253; (c) P. Lara, K. Philippot and B. Chaudret, *ChemCatChem*, 2013, **5**, 28.

4 (a) *Nanocatalysis*, ed. U. Heiz and U. Landman, Springer, Berlin, 2007; (b) *Nanoparticles and catalysis*, ed. D. Astruc, Wiley-VCH, Weinheim, 2008; (c) *Nanomaterials in catalysis*, ed. K. Philippot and P. Serp, Wiley-VCH, Weinheim, 2013.

5 For a recent review, see: L. Wang, W. He and Z. Yu, *Chem. Soc. Rev.*, 2013, **42**, 599.

6 For selected contributions concerning Ni complexes, see: (a) D. A. Vicic and W. D. Jones, *J. Am. Chem. Soc.*, 1997, **119**, 10855; (b) D. A. Vicic and W. D. Jones, *J. Am. Chem. Soc.*, 1999, **121**, 7606; (c) D. Buccella and G. Parkin, *J. Am. Chem. Soc.*, 2008, **130**, 8617; (d) M. R. Grochowski, T. Li, W. W. Brennessel and W. D. Jones, *J. Am. Chem. Soc.*, 2010, **132**, 12412.

7 (a) C. A. Bradley, L. F. Veiros and P. J. Chirik, *Organometallics*, 2007, **26**, 3191; (b) T. Schaub, M. Backes, O. Plietzsch and U. Radius, *Dalton Trans.*, 2009, 7071; (c) S. Kundu, B. E. R. Snyder, A. P. Walsh, W. W. Brennessel and W. D. Jones, *Polyhedron*, 2013, **58**, 99.

8 F. Pan, H. Wnag, P.-X. Shen, J. Zhao and Z. J. Shi, *Chem. Sci.*, 2013, **4**, 1573.

9 (a) A. Nova, F. Novio, P. González-Duarte, A. Lledós and R. Mas-Ballesté, *Eur. J. Inorg. Chem.*, 2007, 5707; (b) H.-M. Wang and E. Iglesia, *ChemCatChem*, 2011, **3**, 1166.

10 J. V. Lauritsen, M. Nyberg, J. K. Norskov, B. S. Clausen, H. Topsoe, E. Laegsgaard and F. Besenbacher, *J. Catal.*, 2004, **224**, 94.

11 S. M. Kane and J. L. Gland, *Surf. Sci.*, 2000, **468**, 101.

12 J. Noh, E. Ito and M. Hara, *J. Colloid Interface Sci.*, 2010, **342**, 513.

13 D. Mott, J. Yin, M. Engelhard, R. Loukrakpam, P. Chang, G. Miller, I.-T. Bae, N. C. Das, C. Wang, J. Luo and C.-J. Zhong, *Chem. Mater.*, 2010, **22**, 261.

14 For FeP nanoparticles, see: (a) J.-H. Chen, M.-F. Tai and K.-M. Chi, *J. Mater. Chem.*, 2004, **14**, 296 for InP nanoparticles, see: (b) P. K. Khama, K.-W. Jun, K. B. Hong, J.-O. Baeg and G. K. Mehrotra, *Mater. Chem. Phys.*, 2005, **92**, 54.

15 I. Amor, M. E. García, M. A. Ruiz, D. Sáez, H. Hamidov and J. C. Jeffery, *Organometallics*, 2006, **25**, 4857.

16 (a) M. J.-L. Tschan, F. Cherioux, L. Karmazin-Brelot and G. Suess-Fink, *Organometallics*, 2005, **24**, 1974; (b) S. Kandala, C. Hammons, W. H. Watson, X. Wang and M. G. Richmond, *Dalton Trans.*, 2010, **39**, 1620; (c) X. Tan, B. Li, S. Xu, H. Song and B. Wang, *Organometallics*, 2011, **30**, 2308.

17 (a) S. E. Kabir, Md. A. Miah, N. C. Nitai, G. M. G. Hussain, K. I. Hardcastle, E. Nordlander and E. Rosengberg, *Organometallics*, 2005, **24**, 3315; (b) W.-Y. Yeh and K.-Y. Tsai, *Organometallics*, 2010, **29**, 604.

18 Md. N. Uddin, M. A. Mottalib, N. Begum, S. Ghosh, A. K. Raha and D. T. Haworth, *Organometallics*, 2009, **28**, 1514.

19 Md. N. Uddin, N. Begum, M. R. Hassan, G. Hogarth, S. E. Kabir, Md. A. Miah, E. Nordlander and D. A. Tocher, *Dalton Trans.*, 2008, 6219.

20 For a significant contribution, see: C. Pan, K. Pelzer, K. Philippot, B. Chaudret, F. Dassenoy, P. Lecante and M.-J. Casanove, *J. Am. Chem. Soc.*, 2001, **123**, 7584.

21 (a) C. Amatore, A. Fuxa and A. Jutand, *Chem. – Eur. J.*, 2000, **6**, 1474; (b) C. Amatore, G. Broeker, A. Jutand and F. Khalil, *J. Am. Chem. Soc.*, 1997, **119**, 5176.

22 J. Real, E. Prat, A. Polo, A. Alvarez-Larena and J. F. Piniella, *Inorg. Chem. Commun.*, 2000, **3**, 221.

23 A. P. Umpierre, G. Machado, G. H. Fecher, J. Morais and J. Dupont, *Adv. Synth. Catal.*, 2005, **347**, 1404.

24 (a) X. Feng, Z. Zhao, F. Yang, T. Jin, Y. Ma and M. Bao, *J. Organomet. Chem.*, 2011, **696**, 1479; (b) M. C. Militello and S. J. Simko, *Surf. Sci. Spectra*, 1994, **3**, 387; (c) C. D. Wagner, A. V. Naumking, A. Kraut-Vass and J. W. Allis, *NIST X-ray Photoelectron Spectroscopy Database, NIST Standar Reference Database 20, V. 4.1 (Web version)* http://srdata.nist.gov/xps/, (July 2013).

25 (a) G. Corthey, A. A. Rubert, A. L. Picone, G. Casillas, L. J. Giovanetti, J. M. Ramallo-López, E. Zelaya, G. A. Benitez, R. G. Requejo, M. José-Yacamán, R. C. Salvarezza and M. H. Fonticelli, *J. Phys. Chem. C*, 2012, **116**, 9830; (b) D. Nilsson, S. Watcharinyanon, M. Eng, L. Li, E. Moons, L. S. Os Johansson, M. Zharnikov, A. Shaporenko, B. Albinsson and J. Martensson, *Langmuir*, 2007, **23**, 6170.

26 I. Tello-López, PhD thesis, Universitat Autònoma de Barcelona, 2010.

27 A. M. López-Vinasco, M. Bruce, P. Gónzalez-Aguirre, A. Rosas-Hernández, C. Amador-Bedolla and E. Martin, *Synthesis*, 2010, 4101.

28 *SDP v4.1 (32 bit) Copyright 2004*, XPS International, LLC, Compiled January 17 2004.

29 J. H. Scofield, *J. Electron Spectrosc. Relat. Phenom.*, 1976, **8**, 129 [Lawrence Livermore Lab work with tabulated values].

30 F. G. Mann and D. Purdie, *J. Chem. Soc.*, 1935, 1549.

31 (*a*) S. V. Vasilyeva, M. A. Vorotyntsev, I. Bezverkhyy, E. Lesniewska, O. Heintz and R. Chassagnon, *J. Phys. Chem. C*, 2008, **112**, 19878; (*b*) K. M. Deshmukh, Z. S. Qureshi, K. D. Bhatte, K. A. Venkatesan, T. G. Srinivasan, P. R. Vasudeva-Rao and B. M. Bhanage, *New J. Chem.*, 2011, **35**, 2747; (*c*) L. Li, J. Wang, T. Wu and R. Wang, *Chem. – Eur. J.*, 2012, **18**, 7842.